ON THE FALSE ALARM PROBABILITY OF THE NORMALIZED MATCHED FILTER FOR OFF-GRID TARGET DETECTION

P. Develter[1,2]   *J. Bosse*[1]   *O. Rabaste*[1]   *P. Forster*[3]   *J.-P. Ovarlez*[1,2]

[1] DEMR, ONERA, Université Paris-Saclay, F-91120 Palaiseau, France
[2] SONDRA, CentraleSupélec, Université Paris-Saclay, F-91192 Gif-sur-Yvette, France
[3] Université Paris-Saclay, ENS Paris-Saclay, CNRS, SATIE, F-91190, Gif-sur-Yvette, France.

ABSTRACT

Off-grid targets are known to induce a mismatch that dramatically impacts the detection probability of the popular Normalized Matched Filter. To overcome this problem, the unknown target parameter is usually estimated through a Maximum Likelihood strategy resulting in a GLRT detection scheme. While the test statistic for the null hypothesis is well known in the on-grid case, the off-grid scenario is more involved and, to the best of our knowledge, no such theoretical result is available. This paper fills this gap by proposing such an expression under circular compound Gaussian noise with known covariance matrix thanks to a geometrical approach.

Index Terms— Radar detection, Off-Grid, GLRT, P_{FA}-threshold relationship, Theory of Tubes

1. INTRODUCTION

Classically, detection of signals with unknown parameters are addressed with a Generalized Likelihood Ratio test (GLRT) that replaces the unknown parameters with their Maximum Likelihood estimators (MLE) in the Likelihood Ratio detection test [1]. When analytical MLE solutions are not available for signal parameters of interest, most detection strategies assume for ease of implementation that those parameters lie over a discrete set, called the grid. However, parameters have no reason to fall precisely on the grid, since they are distributed over a continuous range. This induces a mismatch between the tested parameters and the true target parameters that deteriorates the detection performance of most state-of-the-art tests made under the on-grid assumption. In this paper, we illustrate this problem in the radar context where unknown parameters can include Doppler shift, distance, or direction.

The off-grid impact is particularly dramatic for detection schemes like the Normalized Matched Filter (NMF) test [2]. This test is used under Gaussian noise of unknown level. It is also widely used for adaptive radar in non-Gaussian contexts [3] for example, when the noise is distributed according to a Complex Elliptically Symmetric (CES) distribution [4]. In some cases, the detection probability may vanish to 0 even for high Signal to Noise ratio (SNR) [2], especially for low

P_{FA}, familiar to Radar context. To overcome this problem, the most obvious solution consists in testing over the whole continuous parameter support, not just the grid: this is the true off-grid GLRT. However, to the best of our knowledge, the analytical expression of the null hypothesis statistic and the related P_{FA} is unknown in the literature for this GLRT.

Some works provide optimal analytical solutions for other particular mismatches [5–7], as such they are not optimal for our specific mismatch. Other approaches include approximating the off-grid GLRT, either with a subspace approach [2] or a Monopulse-inspired method [8]. Those solutions are suboptimal: they are designed for practical conditions where the use of a refined, precise approximation of the GLRT is unrealistic because its lack of closed-form can lead to high computational cost. In this paper, we present a derivation of a P_{FA}-threshold relationship for the off-grid NMF. It allows an insightful geometrical analysis of the problem. It is valid for low P_{FA} of interest in common applications.

Section 2 presents the signal model, the off-grid problem and the true GLRT formulation. Section 3 gives the derivation of the P_{FA}-threshold relationship. In Section 4 we check the validity of our derivation by comparing the theoretical thresholds to Monte-Carlo simulations.

Notations: Matrices are in bold and capital, vectors in bold. For any matrix $\mathbf{A}$ or vector, $\mathbf{A}^T$ is the transpose of $\mathbf{A}$ and $\mathbf{A}^H$ is the Hermitian transpose of $\mathbf{A}$. $\mathbf{I}$ is the $N \times N$ identity matrix and $\mathcal{CN}(\boldsymbol{\mu}, \boldsymbol{\Gamma})$ is the circular complex Normal distribution of mean $\boldsymbol{\mu}$ and covariance matrix $\boldsymbol{\Gamma}$. S^{n-1} is the unit sphere in $\mathbb{R}^n$. The real part operator of a complex number is denoted by $\mathrm{Re}(.)$. The operator $\underline{u}$ is the angle of a complex number u.

2. PROBLEM FORMULATION

In radar detection, the main problem consists in detecting a complex signal $\mathbf{d} \in \mathbb{C}^N$ corrupted by an additive noise $\mathbf{n}$ (clutter, thermal noise, etc.). This problem can be stated as the following binary hypothesis test:

$$\begin{cases} H_0 : \mathbf{r} = \mathbf{n}\,, \\ H_1 : \mathbf{r} = \alpha\, \mathbf{d}(\boldsymbol{\theta}) + \mathbf{n}\,, \end{cases} \tag{1}$$
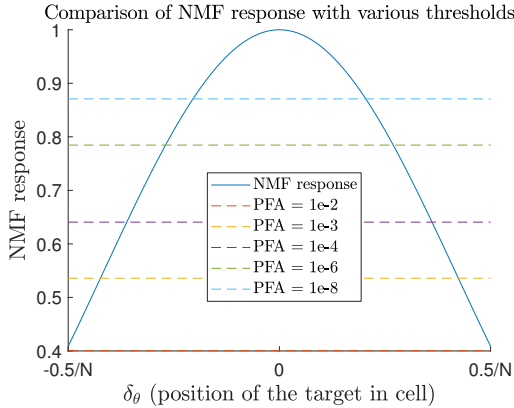
ICASSP 2022

where $\mathbf{r}$ is the complex N-vector of the sampled received signal, α is an unknown complex target amplitude and $\mathbf{d}(\boldsymbol{\theta})$ stands for a generally known *steering vector* characterized by unknown target parameters $\boldsymbol{\theta}$ (time-delay, Doppler or angle). In the sequel, we will assume $\mathbf{n}$ is a zero-mean complex circular Gaussian noise vector with unknown variance σ^2 i.e. $\mathbf{n} \sim \mathcal{CN}(\mathbf{0}, \sigma^2 \boldsymbol{\Gamma})$. This context is known as a partially homogeneous Gaussian environment. Without loss of generality, we will here assume θ to be the scalar Doppler shift of the target and we here investigate only the normalized Doppler steering vector $\mathbf{d}(\theta)$:

$$\mathbf{d}(\theta) = \frac{1}{\sqrt{N}} \left[1, e^{2i\pi\theta}, \dots, e^{2i\pi(N-1)\theta} \right]^T . \tag{2}$$

This model of steering vector is often encountered in radar Range-Doppler detection schemes where the problem consists in estimating a complex sinusoid embedded in noise after range Matched Filter processing.

For unknown parameters $\{\boldsymbol{\lambda}_i\}_{i \in [0,1]}$ depending on each hypothesis $\{H_i\}_{i \in [0,1]}$ (either parameters of interest and/or nuisance parameters), the usual procedure relies on the Generalized Likelihood Ratio (GLR) statistic, namely the ratio $\Lambda(\mathbf{r})$ between the Probability Density Function (PDF) $f_{H_1}(.)$ of the data under H_1 and the PDF $f_{H_0}(.)$ under H_0 where the unknown parameters are replaced by their ML estimate and where w^2 is the detection threshold:

$$\Lambda(\mathbf{r}) = \frac{\max\limits_{\boldsymbol{\lambda}_1} f_{H_1}(\mathbf{r})}{\max\limits_{\boldsymbol{\lambda}_0} f_{H_0}(\mathbf{r})} \overset{H_1}{\underset{H_0}{\gtrless}} w^2. \tag{3}$$

Comparison of NMF response with various thresholds

Fig. 1. Comparison of the NMF response with various thresholds $w^2 = 1 - P_{FA}^{1/(N-1)}$ when $N = 10$, in cell $\mathcal{D} = [-0.5/N, 0.5/N]$.

When $\boldsymbol{\lambda}_1 = \{\alpha, \sigma\}$ and $\boldsymbol{\lambda}_0 = \{\sigma\}$ with θ known, the corresponding GLRT is known as the NMF (Normalized Matched Filter) [9, 10]:

$$\frac{\left| \mathbf{d}(\theta)^H \boldsymbol{\Gamma}^{-1} \mathbf{r} \right|^2}{\left(\mathbf{d}(\theta)^H \boldsymbol{\Gamma}^{-1} \mathbf{d}(\theta) \right) \left(\mathbf{r}^H \boldsymbol{\Gamma}^{-1} \mathbf{r} \right)} \overset{H_1}{\underset{H_0}{\gtrless}} w^2. \tag{4}$$

This test is also widely used for adaptive radar in non-Gaussian contexts [3, 11] for example when the noise is distributed according to a Complex Elliptically Symmetric (CES) distribution [4]. Its statistic in this case is the same as in the Gaussian case.

Equivalently, Eq. (4) can be rewritten with normalized whitened vectors:

$$\left| \mathbf{s}(\theta)^H \mathbf{u} \right|^2 \overset{H_1}{\underset{H_0}{\gtrless}} w^2 , \tag{5}$$

where $\mathbf{s}(\theta) = \dfrac{\boldsymbol{\Gamma}^{-1/2} \mathbf{d}(\theta)}{\left\| \boldsymbol{\Gamma}^{-1/2} \mathbf{d}(\theta) \right\|}$ and $\mathbf{u} = \dfrac{\boldsymbol{\Gamma}^{-1/2} \mathbf{r}}{\left\| \boldsymbol{\Gamma}^{-1/2} \mathbf{r} \right\|}$.

The corresponding P_{FA}-threshold relationship is well known:

$$P_{FA} = \left(1 - w^2 \right)^{N-1} . \tag{6}$$

When the point θ where the NMF is tested is different from the true parameter θ_0 of the target, the target is said to be off-grid. This induces a mismatch ($\theta \neq \theta_0$) between the real target steering vector $\mathbf{s}(\theta)$ and the steering vector $\mathbf{s}(\theta_0)$ under test. Unfortunately, it was shown in [12] that the NMF detector is very sensitive to steering vector mismatch, potentially leading to a dramatic deterioration of the detection performance: in particular for a mismatch larger than the detection threshold, the asymptotic detection probability tends to 0 at high SNR: this phenomenon occurs [2] for P_{FA} as high as 10^{-3} in the chosen resolution cell of width $1/N$. This can be seen in Figure 1 which displays the NMF response without any noise as a function of the mismatch: this response falls below the detection thresholds at the edge of the cell. To correct this issue, θ must be estimated.

When θ is unknown, the natural GLRT procedure leads to

$$GLRT(\mathbf{u}, \mathcal{D}) = \max_{\theta \in \mathcal{D}} \left| \mathbf{s}(\theta)^H \mathbf{u} \right|^2 \overset{H_1}{\underset{H_0}{\gtrless}} w^2 , \tag{7}$$

where $\mathcal{D}$ is the search domain relative to the unknown parameter θ. This detector corrects the off-grid issue of test (5) pointed out in Figure 1. Unfortunately, as of now, no analytical P_{FA}-threshold relationship is known, the difficulty consisting here to evaluate the statistics of the maximum of a continuum of non-independent random variables.

In the next section, we propose to fill this gap.

3. AN ANALYTICAL P_{FA}-THRESHOLD RELATIONSHIP WITH A GEOMETRICAL INTERPRETATION

Through geometrical considerations, Hotelling [13] derived a methodology to study statistical tests over the real sphere. Remarkably, it can be used to evaluate the P_{FA} of the GLRT in the real case: his insightful approach is presented in Section 3.1. Unfortunately, as will be explained in Section 3.2, his derivation cannot be directly transposed to the complex case expressed in (5).

3.1. Hotelling's geometrical approach in the real case

Following Hotelling, let us see how finding a threshold guaranteeing a certain P_{FA} reduces to a simple geometrical problem in the real case, that is, when replacing $\mathbb{C}$ with $\mathbb{R}$ in the previous section.

First, note that the NMF expression (5) has a simple geometrical interpretation. It is indeed the squared cosine of the angle between the normalized steering vector under test $\mathbf{s}(\theta)$ and the normalized whitened received signal $\mathbf{u}$. The threshold can be seen as the squared cosine of the angle $\cos^{-1} w$. When the vectors angle is below this limit angle, a target is detected. Since $\mathbf{u}$ has been whitened, it is uniformly distributed over the unit N-sphere under the null hypothesis.

Thanks to this distribution, we can compute the P_{FA} of the NMF test given in Eq. (5). Let us consider the spherical cap $\mathcal{SC}_\theta^+$ defined by all vectors $\mathbf{u}$ on the sphere verifying $\mathbf{u}^T \mathbf{s}(\theta) < w$ and its symmetric version $\mathcal{SC}_\theta^-$ satisfying $-\mathbf{u}^T \mathbf{s}(\theta) < w$. Let us define $\mathcal{SC}_\theta = \mathcal{SC}_\theta^+ \bigcup \mathcal{SC}_\theta^-$ as the union of the two previous spherical caps. A false alarm occurs as soon as $\mathbf{u} \in \mathcal{SC}_\theta$. Therefore, the P_{FA} is the ratio between the spherical caps surface and the surface of the unit sphere.

Let us now consider the GLRT in Eq. (7). A false alarm occurs when $\mathbf{u} \in \mathcal{T} = \bigcup_{\theta \in \mathcal{D}} \mathcal{SC}_\theta$. Therefore the P_{FA} is the ratio of the surface of $\mathcal{T}$ and the surface of the unit sphere. An example in $\mathbb{R}^3$ is represented in Figure 2 on S^2. Note that $\mathcal{T}$ is the union of two symmetric tubes embedded in the sphere, with geodesic radius $\cos^{-1} w$ around the two curves $\mathbf{s}(\theta)$ and $-\mathbf{s}(\theta)$ with added semi-spherical caps at the ends. $\mathcal{T}$ can thus be written into two equivalent forms [14]:

$$
\begin{aligned}
\mathcal{T} &= \left\{ \mathbf{u} \in S^{N-1} : \max_{\theta \in \mathcal{D}} \left| \mathbf{s}(\theta)^T \mathbf{u} \right| > w \right\} \\
&= \bigcup_{\beta = \pm 1} \left\{ \mathbf{u} \in S^{N-1} : \min_{\theta \in \mathcal{D}} \| \beta \mathbf{s}(\theta) - \mathbf{u} \| < \sqrt{2(1-w)} \right\}.
\end{aligned}
$$

With this form, computing the P_{FA} amounts to finding the surface of the set of points in S^{N-1} that lie at a Euclidean distance $\sqrt{2(1-w)}$ of the curves.

In [13], Hotelling derives an analytical formula for the surface of tubes on the real n-dimensional sphere S^{n-1}.

Theorem 3.1 [13] *The surface enclosed by a tube of geodesic radius ψ around a curve on the real unit sphere S^{n-1} is the product of the length of the axial curve by*

$$
\frac{\pi(n-2)}{2\Gamma\left(\frac{n}{2}\right)} \sin^{n-2}(\psi). \tag{8}
$$

It can be noted that this formula only holds when the considered tubes do not overlap [13]. Overlap phenomenons can happen when the tubes draw back into themselves, or when their curvature becomes too high relative to their radius (local overlap). Non-overlap is locally guaranteed when $\psi =$
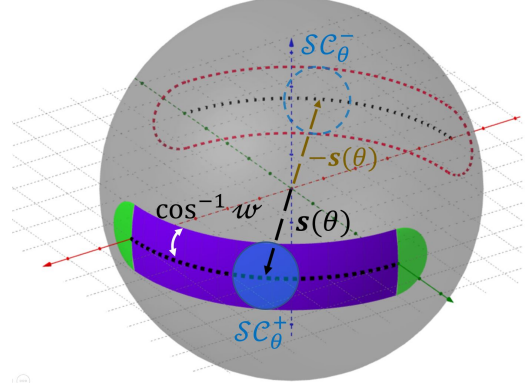
Fig. 2. $\mathcal{T}$ embedded on the unit sphere S^2 in $\mathbb{R}^3$ composed of a tube (in violet) around a one dimensional manifold $\bigcup_{\theta \in \mathcal{D}} \mathbf{s}(\theta)$, two end semi-spherical caps (in green) and their opposite whose outline is dashed. $\mathcal{SC}_\theta$ is drawn in blue. [15]

$\cos^{-1} w$ becomes low enough. In case of overlap, Eq. (8) becomes an upper bound. By adding the surface of the end caps to (8), one can find the surface of $\mathcal{T}$ in the real case.

3.2. Extending Hotelling's approach to the complex case

Unfortunately Hotelling's result is not immediately applicable to the considered GLRT. As we will see, when transposing our complex problem in $\mathbb{R}^{2N}$ the resulting manifold becomes now two-dimensional since the absolute value in the right hand term of the GLRT given in Eq. (7) then implies a search of the maximum on the phase as well.

Indeed, for any real scalar $\alpha \in [0, 2\pi]$, let us remark that $\operatorname{Re}(\mathbf{s}(\theta)^H \mathbf{u} e^{-i\alpha}) \leq \left| \mathbf{s}(\theta)^H \mathbf{u} \right|$, those two quantities being equal for $\alpha = \angle \mathbf{s}(\theta)^H \mathbf{u}$. We then have, decomposing $\mathbf{s}(\theta) = \mathbf{s}_r(\theta) + i \mathbf{s}_i(\theta)$ and $\mathbf{u} = \mathbf{u}_r + i \mathbf{u}_i$ into real and complex parts:

$$
\begin{aligned}
\operatorname{Re}(\mathbf{s}(\theta)^H \mathbf{u} e^{-i\alpha}) &= \left(\mathbf{s}_r(\theta)^T \mathbf{u}_r + \mathbf{s}_i(\theta)^T \mathbf{u}_i \right) \cos\alpha \\
&\quad + \left(\mathbf{s}_r(\theta)^T \mathbf{u}_i - \mathbf{s}_i(\theta)^T \mathbf{u}_r \right) \sin\alpha \\
&= \left(\boldsymbol{\gamma}_1(\theta)^T \underline{\mathbf{u}} \right) \cos\alpha + \left(\boldsymbol{\gamma}_2(\theta)^T \underline{\mathbf{u}} \right) \sin\alpha,
\end{aligned}
$$

where $\boldsymbol{\gamma}_1(\theta) = \begin{bmatrix} \mathbf{s}_r(\theta) \\ \mathbf{s}_i(\theta) \end{bmatrix}, \boldsymbol{\gamma}_2(\theta) = \begin{bmatrix} -\mathbf{s}_i(\theta) \\ \mathbf{s}_r(\theta) \end{bmatrix}$ and $\underline{\mathbf{u}} = \begin{bmatrix} \mathbf{u}_r \\ \mathbf{u}_i \end{bmatrix}$ is a $2N$-real valued noise vector drawn uniformly on S^{2N-1} under H_0. The GLRT (7) can then be written as:

$$
\max_{\alpha,\theta} \left[\left(\boldsymbol{\gamma}_1(\theta)^T \underline{\mathbf{u}} \right) \cos\alpha + \left(\boldsymbol{\gamma}_2(\theta)^T \underline{\mathbf{u}} \right) \sin\alpha \right] \underset{H_0}{\overset{H_1}{\gtrless}} w. \tag{9}
$$

The two-dimensional nature of the so-defined real manifold to inspect is directly apparent with this formulation. Indeed, by denoting $\boldsymbol{\gamma}(\alpha, \theta) = \boldsymbol{\gamma}_1(\theta) \cos\alpha + \boldsymbol{\gamma}_2(\theta) \sin\alpha$, the acceptance region in the complex case is a new tube $\mathcal{T}$ around the two-dimensional manifold $\boldsymbol{\gamma}(\theta, \alpha)$:

$$\mathcal{T} = \left\{ \underline{\mathbf{u}} \in S^{2N-1} : \max_{\theta \in \mathcal{D}, \alpha} \gamma(\theta, \alpha)^T \underline{\mathbf{u}} > w \right\}$$

$$= \left\{ \underline{\mathbf{u}} \in S^{2N-1} : \min_{\theta \in \mathcal{D}, \alpha} \| \gamma(\theta, \alpha) - \underline{\mathbf{u}} \| < \sqrt{2(1-w)} \right\}.$$

Hotelling's result does not cover this multi-dimensional manifold case as it gives the surface of a tube around a curve. However, in [14] and [16], this result is extended to a special case of two-dimensional manifolds which is of interest to us:

Theorem 3.2 [14] *For $i \in [1, 2]$, let $\gamma_i : [0, t_0] \to S^{n-1}$ be regular curves. Assume $\gamma_1(t)^T \gamma_2(t) = 0$ for all t. Let $Z(t) = \left[\left(\gamma_1(t)^T \mathbf{u} \right)^2 + \left(\gamma_2(t)^T \mathbf{u} \right)^2 \right]^{1/2}$ where $\mathbf{u}$ is uniformly distributed on S^{n-1}. Then for $0 < w < 1$, we have:*

$$\mathbb{P}\left(\max_{0 \le t \le t_0} Z(t) > w \right) \le (1 - w^2)^{(n-2)/2} +$$

$$\frac{\Gamma\left(\dfrac{n}{2}\right) w \left(1 - w^2\right)^{(n-3)/2}}{2\pi^{3/2} \Gamma\left(\dfrac{n-1}{2}\right)} \times$$

$$\int_0^{t_0} \int_0^{2\pi} \left[\| \dot{\gamma}_1(t) \cos\omega + \dot{\gamma}_2(t) \sin\omega \|^2 - \left(\dot{\gamma}_1(t)^T \gamma_2(t) \right)^2 \right]^{1/2} d\omega \, dt, \quad (10)$$

where $\dot{\gamma}_i(t)$ is the derivative of $\gamma_i(t)$ with respect to t. When there is no overlap, this inequality becomes an equality.

It turns out that we can reformulate our problem in order to fulfill the assumptions of the above theorem. With our notations, it is easy to check that

$$\left| \mathbf{s}(\theta)^H \mathbf{u} \right|^2 = \left| \gamma_1(\theta)^T \underline{\mathbf{u}} \right|^2 + \left| \gamma_2(\theta)^T \underline{\mathbf{u}} \right|^2, \quad (11)$$

so that Theorem 3.2 gives us the desired P_{FA} (when the equality holds). Follows our main result:

Corollary 3.2.1 *In the absence of overlap (low P_{FA} regimes), the P_{FA} for the GLRT (7) for a search interval $\mathcal{D} = [\theta_1, \theta_2]$ with the steering vector $\mathbf{d}(\theta)$ defined in (2) is given by:*

- *Under white noise ($\Gamma = \sigma^2 \mathbf{I}$):*

$$P_{FA} = (1 - w^2)^{N-1} + \quad (12)$$
$$\sqrt{\frac{\pi}{3}} \frac{\Gamma(N) w (1 - w^2)^{N-\frac{3}{2}}}{\Gamma\left(N - \frac{1}{2}\right)} \left(N^2 - 1\right)^{\frac{1}{2}} (\theta_2 - \theta_1).$$

- *Under colored noise ($\Gamma \neq \sigma^2 \mathbf{I}$), the integral in (10) can be evaluated numerically.*

The first term in (12) represents the surface of the two semi-spherical caps at the extremities of the tube. As such, it is equal to the known P_{FA} of the NMF expressed in Eq. (6). The second term shows the influence of the manifold induced
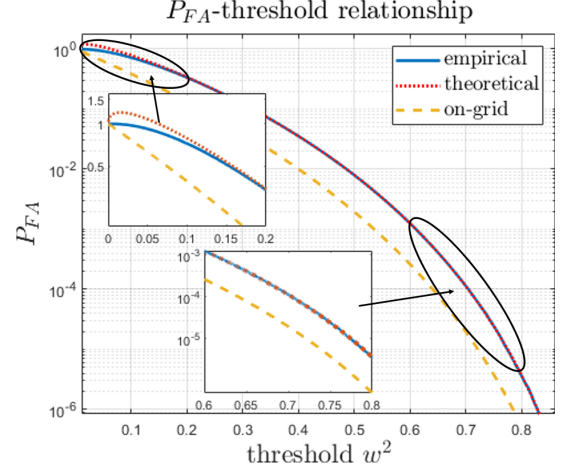
Fig. 3. Comparison between the theoretical P_{FA}-threshold given in (12) and the empirical Monte Carlo P_{FA}-threshold relationships for $N = 10$. The on-grid relation (6) is also drawn for comparison purposes. Tests in the cell [0/N , 1/N].

by the off-grid nature of the problem. It is analogous to the one-dimensional case of Theorem 3.1, where the surface of the cross-section is multiplied by the length of the manifold. Here, $\theta_2 - \theta_1$ plays the role of the manifold length, and the rest of the rightmost term is the surface of the cross-section.

4. NUMERICAL RESULTS

Let us check the validity of the formula (12). Figure 3 presents the P_{FA}-threshold relationship given by Eq. (12) and empirically computed thresholds using 10^8 complex circular white Gaussian noise samples for a steering vector size of $N = 10$. The continuous research over the domain $\mathcal{D}$ is replaced by a discrete search using 30 tests, where $\mathcal{D} = [0, 1/N]$ is one of the usual Fourier resolution cells.

The formula fits perfectly when the P_{FA} is low enough (or, equivalently, if the threshold is high enough). The formula is not valid for P_{FA} close to 1 because of overlap (it even exceeds 1). However, such high P_{FA} have no practical interest for common applications. A detailed analysis of overlap phenomena will be given in a subsequent paper.

5. CONCLUSION

In this paper, we addressed the off-grid detection problem using the NMF-GLRT by finding an analytical P_{FA}-threshold relationship, valid for most common applications. In future works, we will mathematically investigate the conditions guaranteeing that no overlap is present for a given P_{FA} value. This will enable us to provide the precise domain and the conditions under which our relationship is valid.

6. REFERENCES

[1] L. L. Scharf and C. Demeure, *Statistical signal processing: detection, estimation, and time series analysis*, Prentice Hall, 1991.

[2] O. Rabaste, J. Bosse, and J-P. Ovarlez, "Off-grid target detection with Normalized Matched Subspace Filter," in *24th European Signal Processing Conference (EUSIPCO)*, aug 2016, pp. 1926–1930.

[3] F. Pascal, J.-P. Ovarlez, P. Forster, and P. Larzabal, "On a SIRV-CFAR detector with radar experimentations in impulsive noise," in *European Signal Processing Conference, EUSIPCO'06*, Florence, Italy, September 2006.

[4] E. Ollila, D. E. Tyler, V. Koivunen, and H. V. Poor, "Complex Elliptically Symmetric distributions: Survey, new results and applications," *Signal Processing, IEEE Transactions on*, vol. 60, no. 11, pp. 5597 –5625, nov. 2012.

[5] O. Besson, "Detection of a signal in linear subspace with bounded mismatch," *Aerospace and Electronic Systems, IEEE Transactions on*, vol. 42, no. 3, pp. 1131–1139, 2006.

[6] F. Bandiera, D. Orlando, and G. Ricci, *Advanced Radar Detection Schemes Under Mismatched Signal Models*, Morgan & Claypool publishers, 2009.

[7] A. De Maio, Y. Huang, D. P. Palomar, S. Zhang, and A. Farina, "Fractional QCQP with applications in ML steering direction estimation for radar detection," *Signal Processing, IEEE Transactions on*, vol. 59, no. 1, pp. 172–185, 2010.

[8] P. Develter, J. Bosse, O. Rabaste, P. Forster, and J.-P. Ovarlez, "Off-grid radar target detection with the normalized matched filter: A monopulse-based detection scheme," in *2021 IEEE Statistical Signal Processing Workshop (SSP)*. IEEE, 2021, pp. 226–230.

[9] L. L. Scharf and D. W. Lytle, "Signal detection in Gaussian noise of unknown level: an invariance application," *Information Theory, IEEE Transactions on*, vol. 17, pp. 404–411, July 1971.

[10] L. L. Scharf and B. Friedlander, "Matched subspace detectors," *Signal Processing, IEEE Transactions on*, vol. 42, no. 8, pp. 2146–2157, 1994.

[11] E. Conte, M. Lops, and G. Ricci, "Asymptotically optimum radar detection in compound-Gaussian clutter," *Aerospace and Electronic Systems, IEEE Transactions on*, vol. 31, no. 2, pp. 617–625, April 1995.

[12] O. Rabaste and N. Trouvé, "Geometrical design of radar detectors in moderately impulsive noise," *Aerospace and Electronic Systems, IEEE Transactions on*, vol. 50, no. 3, pp. 1938–1954, 2014.

[13] H. Hotelling, "Tubes and spheres in n-spaces, and a class of statistical problems," *American Journal of Mathematics*, vol. 61, no. 2, pp. 440–460, 1939.

[14] I. Johnstone and D. Siegmund, "On Hotelling's formula for the volume of tubes and Naiman's inequality," *The Annals of Statistics*, pp. 184–194, 1989.

[15] M. Hohenwarter, *GeoGebra - ein Softwaresystem für dynamische Geometrie und Algebra der Ebene*, 2002, Diplomarbeit, Universität Salzburg.

[16] M. Knowles and D. Siegmund, "On Hotelling's approach to testing for a nonlinear parameter in regression," *International Statistical Review/Revue Internationale de Statistique*, pp. 205–220, 1989.